Formation of Local Native-like Tertiary Structures in the Slow Refolding Reaction of Human Carbonic Anhydrase II as Monitored by Circular Dichroism on Tryptophan Mutants†

Dick Andersson,‡ Per-Ola Freskgård,‡,§ Bengt-Harald Jonsson,‖ and Uno Carlsson*,‡

IFM-Department of Chemistry, Linköping University, S-581 83 Linköping, Sweden, and Department of Biochemistry, Umeå University, S-901 87 Umeå, Sweden

Received August 5, 1996; Revised Manuscript Received December 12, 1996⊗

ABSTRACT: In the present study, near-UV CD kinetic measurements on mutants, in which one Trp residue had been replaced, were performed to probe the development of asymmetric environments around specific Trp residues during the refolding of human carbonic anhydrase II (HCAII). In addition, the formation of the active site was probed by the binding of a fluorescent sulfonamide inhibitor. The development of the individual Trp CD spectra during refolding was obtained by subtracting the CD spectrum of the mutant lacking one Trp from that of HCAII at different time points. The same method was used for the particular Trp residues to obtain the kinetic CD traces monitored at a specific wavelength (270 nm). Trp residues 16, 97, and 245 were analyzed. Trp16 probes the N-terminal domain (amino acid residues 1−25), and this part is forming its tertiary structure slower than the major domain (amino acid residues 26−260) of the protein molecule, which contains the active site and a dominating β-sheet. An essentially native structure of the major domain seems to act as a template for the correct folding of the N terminus. Trp97 is located in a hydrophobic cluster comprising β-strands 3−5 in the protein core. Previously, we have shown that this region is remarkably stable and compact, and stopped-flow fluorescence data indicate that Trp97 is buried in an apolar compact cluster within a few milliseconds [Svensson, M., Jonasson, P., Freskgård, P.-O., Jonsson, B.-H., Lindgren, M., Mårtensson, L.-G., Gentile, M., Borén, K., & Carlsson, U. (1995) *Biochemistry 34*, 8606−8620; Jonasson, P., Aronsson, G., Carlsson, U., & Jonsson, B.-H. (1997) *Biochemistry 36* (in press)]. Here it is shown that the development of the native tertiary structure at Trp97 occurs in the minute time domain. Trp245 is located in a long loop between the N-terminal domain and the core structure. Although this Trp has attained native-like fluorescence properties within the dead time of the CD experiment, it assumes a native-like asymmetric environment even slower than Trp97. Thus, the investigated Trp residues develop their native CD bands at different rates, showing that formation of native-like tertiary structure is occurring with varying rates in different regions of the protein.

The three-dimensional conformation of proteins is essential to their function. To reach the biologically active native state, the polypeptide chain has to fold into a highly condensed form, in which the amino acid residues become packed against each other. These packing interactions, especially in the protein core, have been shown to be essential for both the stability and the activity of proteins (Lim & Sauer, 1991; Sandberg & Terwilliger, 1991). As a consequence, the hydrophobic character of buried amino acid residues in related proteins is highly conserved (Bashford et al., 1987). The amino acid residues are, because of the tight packing, more or less immobilized in specific orientations in the native protein conformation.

A number of questions concerning the packing of the protein structure during the folding process are still left to be answered. How highly packed is the intermediate(s) (molten-globule states) that is formed initially during the folding process? Does the intermediate contain regions with high native-like tertiary order?

A technique that can specifically monitor packing interactions, i.e. asymmetry of structure, is circular dichroism (CD).[1] Individual CD bands in the near-UV region reflect the surroundings of aromatic amino acid residues in the three-dimensional protein structure. These bands are extremely sensitive to changes in the tertiary structure and are often used as a "fingerprint" of the native conformation. In particular, Trp residues have recently been shown to possess strong bands in this region of the CD spectra from the proteins interleukin IL-1β (Craig et al., 1989), barnase (Vuilleumier et al., 1993), and human carbonic anhydrase II (HCAII) (Freskgård et al., 1994). In the case of HCAII, the entire near-UV spectrum could essentially be reconstructed from the individual CD bands of the seven Trp residues in the protein (Freskgård et al., 1994).

† This work was supported by grants from the Swedish National Board for Industrial and Technical Development (88-04439P, U.C.; 88-04439P, B.-H.J.), the Swedish Natural Science Research Council (K-Ku 4241-301, U.C.; K-Ku 9426-300, B.-H.J.), the Sven and Lily Lawskis Fond (P.-O.F.), and the Marcus and Amalia Wallenbergs Minnesfond (U.C.).

* To whom correspondence should be addressed.

‡ Linköping University.

§ Present address: California Institute of Technology, 210-111, Pasadena, CA 91125.

‖ Umeå University.

⊗ Abstract published in *Advance ACS Abstracts,* March 15, 1997.

[1] Abbreviations: CD, circular dichroism; DNSA, 5-(dimethylamino)-naphthalene-1-sulfonamide; GuHCl, guanidine hydrochloride; HCAII, human carbonic anhydrase II; $HCAII_{pwt}$, pseudo-wild type of HCA II.

S0006-2960(96)01925-3 CCC: $14.00

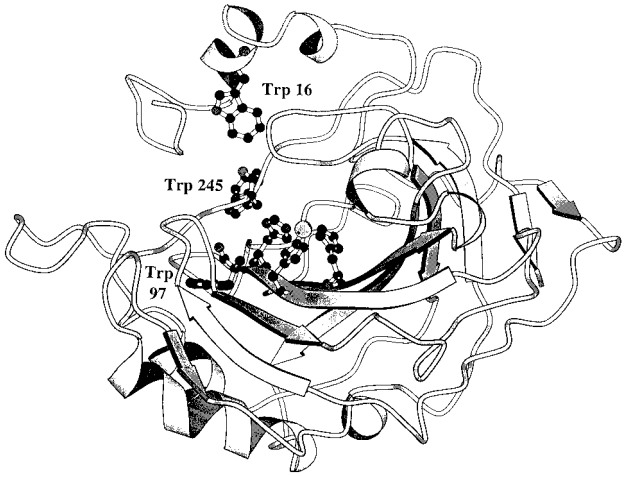

FIGURE 1: Ribbon diagram showing the polypeptide backbone of human carbonic anhydrase II with the major secondary structural elements and residues Trp16, Trp97, and Trp245. The three His ligands coordinating the Zn^{2+} ion in the active site cavity are also included. The diagram has been drawn with the program MolScript (Kraulis, 1991).

HCAII is a monomeric protein of "medium size" consisting of 259 amino acid residues. The crystal structure has been determined at high resolution (Håkansson et al., 1993).

The protein consists of a dominating β-sheet structure, made up by 10 β-strands, that divides the molecule into two halves (Figure 1). Each half contains a hydrophobic cluster, one in the N-terminal region and another large one in the lower half. The active site region is located in the upper half of the structure.

It has previously been demonstrated that HCAII and engineered mutants thereof unfold into two well-separated transitions, indicating the existence of a stable folding intermediate. In this intermediate, β-strands 3−7 appear to have a native-like compact structure (Mårtensson et al., 1992, 1993; Svensson et al., 1995).

In the present study, near-UV CD measurements on engineered mutants lacking one Trp residue were performed to probe the development of asymmetric environments around specific Trp residues during the refolding process of HCAII.

In addition, the formation of the active site was probed by the binding of a fluorescent sulfonamide inhibitor.

MATERIALS AND METHODS

Materials. Sequential grade guanidine hydrochloride (GuHCl) was obtained from Pierce and was made metal-free by extraction with dithiozone (7 mg/L) in carbon tetrachloride. GuHCl concentrations were determined by measuring the index of refraction (Nozaki, 1972). IPTG (isopropyl 1-thio-β-D-galactopyranoside) and DNSA [5-(dimethylamino)naphthalene-1-sulfonamide] were purchased from Sigma. All other chemicals were reagent grade.

Protein Mutagenesis, Production, and Purification. Mutagenesis of HCAII and the production of the protein variants were performed as previously described (Freskgård et al., 1994). One tryptophan residue was replaced by another amino acid residue in three different positions, and the following mutants were constructed: W16F, W97C, and W245C. These variants were purified in a single step using affinity chromatography (Khalifah et al., 1977), and the purity was confirmed by SDS−PAGE. The protein concentration was determined spectrophotometrically at 280 nm using the extinction coefficient 54 800 M^{-1} cm^{-1} for HCAII (Nyman & Lindskog, 1964). Calculation of the extinction coefficients for the mutants according to Gill and von Hippel (1989) resulted in 49 000, 49 000, and 50 400 M^{-1} cm^{-1} for W16F, W97C, and W245C, respectively.

Unfolding and Refolding. In each case, the protein was first unfolded in 5 M GuHCl (0.1 M Tris-H_2SO_4 at pH 7.5) for 1−2 h with a protein concentration of 114 μM. The refolding was initiated by dilution to a final concentration of 0.15 M GuHCl (0.1 M Tris-H_2SO_4 at pH 7.5). The solution was then filtered (Millipore, pore size of 0.8 μm) directly into the used observation cuvette, and the time from mixing to the start of data collection was 60 s. The final protein concentration (approximately 3.4 μM) was determined spectrophotometrically after completion of the refolding process on a Hitachi U2000 spectrophotometer using an identical solution, except the protein, as a reference.

Esterase Activity. The specific esterase activity for hydrolysis of 4-nitrophenyl acetate was determined by using a substrate concentration of 0.5 mM 4-nitrophenyl acetate in 0.1 M Tris-H_2SO_4 (pH 8.0) and 5% acetone; the ionic strength was adjusted to 0.1 M with Na_2SO_4. The reaction was measured spectrophotometrically at 348 nm ($\Delta\epsilon_{348nm}$ = 5000 M^{-1} cm^{-1}), and the apparent second-order rate constant, k', was determined (Thorslund & Lindskog, 1967).

Inhibitor Binding Assay. The formation of the active site in refolding experiments was studied by registration of the binding of the specific carbonic anhydrase inhibitor 5-(dimethylaminonaphthalene-1-sulfonamide (DNSA), from the change in fluorescence intensity at 460 nm (Chen & Kernohan, 1967; Henkens et al., 1982). The measurements were carried out on a Hitachi F-4500 spectrofluorophotometer. The emission band width was 10 nm. The excitation wavelength was 320 nm with a band width of 2.5 nm. The cuvette path length was 1 cm, and the time from mixing and filtration to observation was 60 s. DNSA was used in a 10-fold molar excess (34 μM) over the protein concentration.

CD Measurements. All the kinetic and equilibrium experiments were carried out using the CD6 spectrodichrograph from Jobin-Yvon (Longjumeau, France). The spectra between 255 and 320 nm were recorded by collecting data at 0.5 nm intervals with an integration time of 0.4 s (scan speed of 0.8 nm s^{-1}). The protein concentration of the solution in the CD cuvette was determined after the refolding process was completed. The scanning of the CD spectra was initiated 1 min after the onset of the refolding process. The spectra were run from low to high wavelengths, and the time for collecting the total spectrum was 52 s. Thus, the CD signals at higher wavelengths are of older origin, and the total CD spectrum does not represent one point of time. However, at each specific wavelength, the spectra have developed for equally long times, allowing the ellipticities to be compared. Using a faster scan rate to reduce the spectral change during each scan resulted in an unacceptable low signal to noise ratio.

Each protein spectrum was corrected by subtraction of a spectrum obtained for a solution lacking the protein but otherwise identical. The resulting spectra were smoothed using the minimum filter included in the CD6 software. The kinetic trace at a fixed wavelength was sampled with an interval of 10 s and an integration time of 8 s. The ellipticity

Table 1: Esterase Activity for Reference and Refolded Protein Variants[a]

variant	esterase activity native (k')[b]	filtered[c] refolded (k')	unfiltered[d] refolded (k')
C206S	1460	980 (67)[e]	940 (64)[e]
W16F/C206S	920	720 (78)	710 (77)
W97C/C206S	810	530 (66)	490 (61)
W245C/C206S	1110	720 (64)	700 (63)

[a] The specific activity for esterase hydrolysis in 0.15 M GuHCl was measured using 0.5 mM 4-nitrophenyl acetate as a substrate at pH 8.0. [b] k', in M^{-1} s^{-1}, is the apparent second-order rate constant of the reaction. [c] The samples were filtered immediately after the onset of reactivation. [d] The samples were not filtered after the onset of reactivation. [e] The reactivation percent compared to the native form in 0.15 M GuHCl is shown in parentheses.

is reported as mean residue molar ellipticity ([θ], degree per inverse squared centimeter per mole) and calculated from

$$[\theta] = 10[\theta]_{obs}\text{mrw}cl$$

where $[\theta]_{obs}$ is the ellipticity measured in degrees, mrw is the mean residue molecular weight (molecular weight of 29 300 and 259 amino acid residues), c is the protein concentration (in grams per milliliter), and l is the optical path length of the cell (in centimeters).

Data Analysis. Using a nonlinear least-squares program (TableCurve, Jandel Scientific), kinetic refolding data were fit to a sum of exponential terms.

The refolding data (the refolding spectra and the kinetic traces at 270 nm) were normalized by a factor corresponding to the difference in intensity at 270 nm between the completely refolded protein (2 h) and a reference sample of the native protein. This was done to correct for the less than 100% yield in the refolding experiments and to make it possible to subtract the spectra of the mutants lacking one Trp residue from those of $HCAII_{pwt}$.

RESULTS

The wild-type structure of HCAII contains one Cys residue at position 206. This Cys residue was replaced by a Ser residue to produce a pseudo-wild-type protein, designated $HCAII_{pwt}$, that is completely lacking Cys residues in the protein structure. Earlier, we have shown that $HCAII_{pwt}$ has stability and catalytic ability practically identical with those of the wild-type enzyme (Mårtensson et al., 1995). The $HCAII_{pwt}$ protein was used as a template to create mutants lacking one Trp residue by site-directed mutagenesis. The GuHCl concentration of 0.15 M, which was used in all refolding experiments, is well below the denaturation transition region of all of the mutants, allowing formation of a stable native state. In all experiments, we started to observe the reaction 1 min after the initiation of the refolding; this is the time it took to manually mix and filter the sample.

Specific Enzyme Activity. The specific activity of the native enzymes (k') and reactivation yields were investigated by measuring the esterase activity using 4-nitrophenyl acetate as a substrate. The specific esterase activity of $HCAII_{pwt}$ is 1460 M^{-1} s^{-1} at pH 8.0 (Table 1). For the mutants lacking one Trp residue, the specific esterase activity is lowered by 45% or less compared to that of $HCAII_{pwt}$ (Table 1). This shows that the substitutions of Trp residues cause very minor alterations of the active site, a conclusion that is also supported by measurements of the CO_2 hydration activity of these mutants (Mårtensson et al., 1995). Notably, the esterase and CO_2 hydration activity are affected differently in these mutants, an observation that has also been found for a large number of other mutants of HCAII (Behravan et al., 1991; Krebs & Fierke, 1993). Determination of the reactivation yield of $HCAII_{pwt}$ and of the mutants lacking one Trp was performed by measurement of the esterase activity after 2 h of reactivation. The yield was between 61 and 77% compared to the reference protein (in 0.15 M GuHCl) (Table 1).

In a separate experiment, the protein variants were filtered directly after the initiation of reactivation to remove non-native aggregates from the reactivation solution. Measurement of the protein concentration after the reactivation was completed (2 h) showed that approximately 10−15% of the protein content was removed by the filtration step. However, the reactivation yield increased only slightly compared to that of the unfiltered samples (Table 1), indicating that the filtration discriminates poorly between aggregates and correctly folded molecules. Therefore, only a small fraction of non-native aggregates was removed. This shows either that non-native aggregates are formed at later stages of the refolding process or that the non-native aggregates were too small in size to be removed from the protein solution by filtration. However, an important advantage with the filtration step was the fact that the signal to noise ratio was improved when monitoring the refolding reaction, and it was therefore included before registration of CD spectra and DNSA binding.

Refolding Phases Detected by DNSA Binding. The formation of the active site during the refolding reaction was studied on $HCAII_{pwt}$ and the mutants lacking one Trp residue to investigate the functional significance of the mutated amino acid residues in this process. This was accomplished by measuring the binding of the specific carbonic anhydrase inhibitor, DNSA, to the active site of the protein variants during renaturation. Binding of DNSA results in an increase of the fluorescence emission at 460 nm, allowing us to specifically monitor the folding event leading to a functional active site.

The time course of formation of the active site during refolding is shown for the various protein variants in Figure 2. The formation of the active site is described by two exponential kinetic phases with the rate constants k_1 and k_2 (Table 2).

Development of CD Spectra during Refolding. The CD spectra between 255 and 320 nm were sampled at various times during refolding of $HCAII_{pwt}$ and the mutants lacking one Trp. All CD spectra recorded for the refolding protein variants were normalized by a "yield factor". In each case, these factors were obtained by calculating the ratio of the ellipticity at 270 nm from the spectra of the native protein variants and the spectra of the refolded proteins (2 h). A key question regarding this normalization procedure is, of course, how the inactive protein molecules obtained in the refolding process affect the CD signal. In a control experiment, the active enzyme molecules were separated from the inactive protein, after completion of refolding (2 h), by using affinity chromatography (Khalifah et al., 1977). The CD spectra of the inactive fraction of the refolded molecules did not possess any specific CD bands in the near-UV region (Figure 3A). Therefore, the normalization of the CD spectra with the "yield factor" is justified, since it is reasonable to

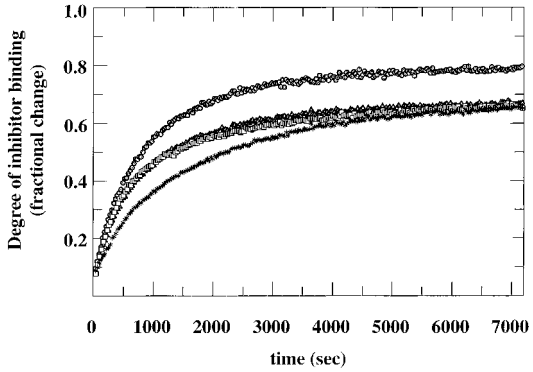

FIGURE 2: Refolding kinetics of formation of a functioning enzyme as monitored by the binding of the inhibitor DNSA to the active site. $HCAII_{pwt}$ and mutants lacking one Trp residue were reactivated from 5 M GuHCl by dilution to 0.15 M GuHCl. The binding of DNSA was monitored by fluorescence measurements as described in Materials and Methods. The kinetic data were best fitted to two exponential terms, and the rate constants are given in Table 2. (▲) $HCAII_{pwt}$, (●) W16F/C206S mutant, (*) W97C/C206S mutant, and (□), W245C/C206S mutant.

Table 2: Kinetic Data for the Formation of a Functional Active Site of $HCAII_{pwt}$ and Tryptophan Mutants Thereof during Refolding as Monitored by DNSA Binding[a]

variant	$k_1{}^b$ ($\times 10^3\ s^{-1}$)	$A_1{}^b$	$k_2{}^b$ ($\times 10^3\ s^{-1}$)	$A_2{}^b$
C206S	2.6 ± 0.1	28 ± 1	0.62 ± 0.01	35 ± 1
W16F/C206S	2.3 ± 0.1	33 ± 1	0.66 ± 0.01	41 ± 1
W97C/C206S	2.7 ± 0.1	14 ± 1	0.47 ± 0.01	48 ± 1
W245C/C206S	2.9 ± 0.1	34 ± 1	0.46 ± 0.01	30 ± 1

[a] The protein variants were denatured in 5 M GuHCl and then refolded by dilution to 0.15 M GuHCl. A 10-fold molar excess of DNSA over enzyme was used. [b] The rate constants and amplitudes were calculated using a nonlinear fit program (see Materials and Methods). The numbers are given with 95% confidence intervals. The amplitudes correspond to the percent of bound DNSA compared to that bound to native $HCAII_{pwt}$.

conclude that the spectra obtained during the refolding process reflect exclusively those protein molecules that are able to fold to the native conformation.

The normalized CD spectra of the various protein variants obtained at different stages during the refolding process are shown in Figure 3A−D. The near-UV CD spectrum of the native $HCAII_{pwt}$ is included in Figure 3A for comparison. As can be seen, the shape of the CD spectrum obtained after 2 h of refolding of $HCAII_{pwt}$ is practically identical to that of the native enzyme in the entire spectral region, indicating that a fully regained native near-UV CD spectrum was achieved for the refolded molecules at these refolding conditions. Corresponding CD spectra of the mutants lacking one Trp were recorded under identical conditions (Figure 3B−D), and the spectra of the native mutants are also included. The CD spectrum of each of the refolded mutant, lacking one Trp residue closely resembled that of the native mutant. This indicates that the tertiary structure of all investigated protein variants is unaltered by the refolding experiment.

The ellipticities of the CD spectra of the unfolded $HCAII_{pwt}$ and the mutants lacking one Trp residue in 5 M GuHCl (Figure 4A−C) were of very low magnitude, indicating substantial flexibility around each Trp residue.

Individual Trp CD Spectra. The CD spectrum of the replaced Trp is calculated by subtracting the spectrum of the mutant lacking one Trp residue from the $HCAII_{pwt}$ spectrum (Freskgård et al., 1994). The individual CD spectra of the Trp residues as they develop during the refolding process are shown in Figure 4A−C. It is clearly shown that Trp16 does not contribute to the CD spectrum above 295 nm during the refolding process (Figure 4A) in contrast to Trp97 and Trp245 (Figure 4B,C). Further, the rate of formation of the Trp97 CD spectrum is fast compared to those of the other two Trp residues.

For all three Trp residues studied in this work, the individual CD spectra seem to develop symmetrically in the entire wavelength region (Figure 4A−C). This observation suggests that the CD signal in the near-UV region is only monitoring the final native state of the probed substructure, because if partially folded substructures are formed CD spectra with a shape different from that of the native state would most probably have evolved.

CD Changes Monitored at 270 nm. To obtain a more detailed kinetic characterization of the refolding process, the kinetics of the recovery of the near-UV CD spectra of $HCAII_{pwt}$ and the mutants lacking one Trp residue during the refolding process were followed at 270 nm (Figure 5), a wavelength at which $HCAII_{pwt}$ has a major CD band (Freskgård et al., 1994). The kinetic experiment was run in quadruplicate for each protein sample to assure that the results were reproducible, and replicate refoldings gave virtually identical results. The mean rate constants and amplitudes were calculated from all collected kinetic data of all investigated protein variants and are shown in Table 3. The time course for one representative refolding reaction is also shown (Figure 5). The symbols in Figure 5 represent values at 270 nm taken from the successively scanned CD spectra during the refolding process (Figure 3). The time points checked show that there is a good experimental agreement between the data obtained from the scanned spectra and the data obtained when monitoring the refolding process continuously at 270 nm.

Using the same method as that for the calculation of the individual Trp CD spectra, it was possible to obtain the individual refolding kinetic CD trace of a specific Trp residue by subtraction of the kinetic trace of the mutant lacking this Trp residue from that of $HCAII_{pwt}$.

The resulting refolding kinetic CD curves of the individual Trp's are shown in Figure 6, and it can be seen that the noise is higher after the subtraction procedure than in the original data; the data could nevertheless be fitted to one or two exponential terms. The calculated mean values of the rate constants from the CD kinetics of each investigated Trp are given in Table 4.

DISCUSSION

Existence of slow kinetic phases after an initial rapid phase is often noticed for medium- to large-sized proteins, when the refolding process is registered by various parameters. Slow kinetic phases are also found for HCAII, which have been shown to, at least partly, be due to *cis*−*trans* isomerization at proline peptide bonds (Fransson et al., 1992). Similar kinetic results have been reported for the structurally closely related bovine CAII (Semisotnov et al., 1990). Since the refolding process of HCAII involves slow steps, the changes in the near-UV region of the CD spectrum upon refolding could be followed after manual mixing by scanning of spectra throughout the reaction. In this study, we have

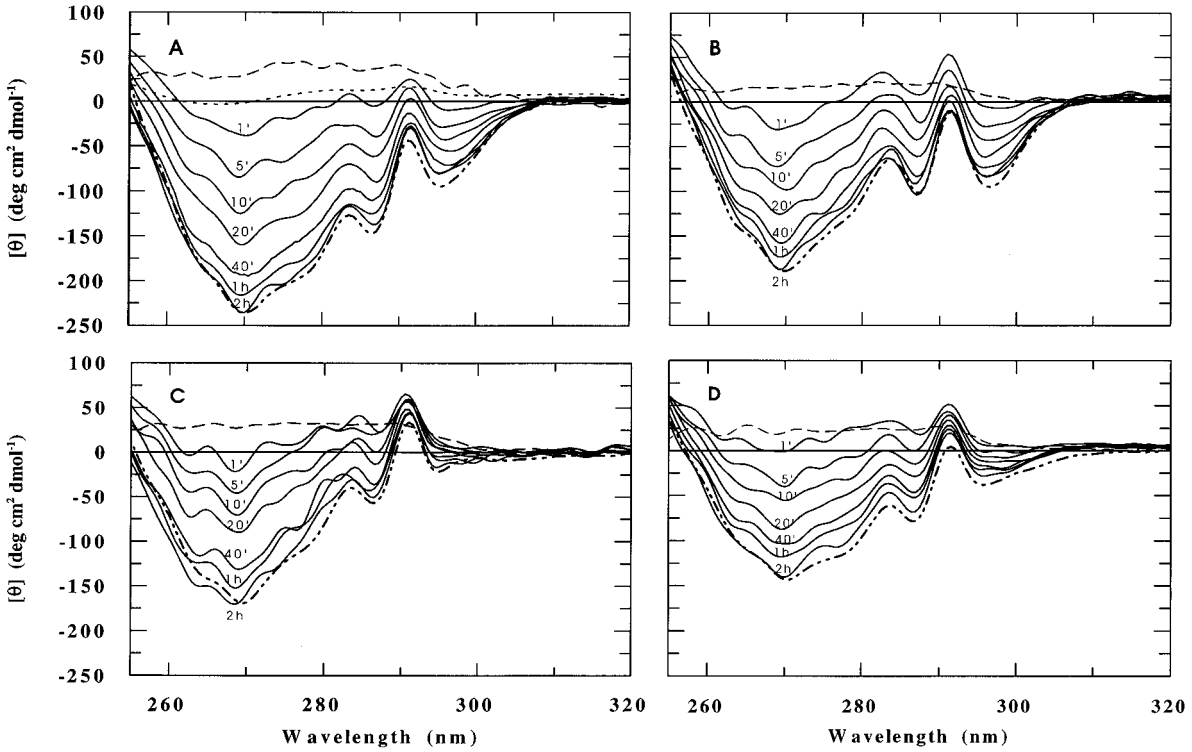

FIGURE 3: Development of near-UV CD spectra for $HCAII_{pwt}$ and mutants lacking one Trp residue during refolding. The time when the scan was started after the onset of refolding is indicated together with each spectrum: (—) refolding protein, (— - - —) native protein, and (- - -) denatured protein (in 5 M GuHCl). The CD spectrum of the inactive part of $HCAII_{pwt}$ (•••) after refolding is also included in panel A: (A) $HCAII_{pwt}$, (B) W16F/C206S mutant, (C) W97C/C206S mutant, and (D) W245C/C206S mutant.

demonstrated that it is, indeed, possible to observe changes in the asymmetric environment of specific Trp residues during the slow stages of the refolding of $HCAII_{pwt}$, by CD. This is possible, although the situation is complex with seven Trp residues in the protein structure.

Three of the seven Trp residues in the protein, Trp16, -97, and -245, were selectively analyzed. These Trp's are located in different regions of the protein structure and have been exploited to probe formation of local ordered structure during the refolding process. Trp16 is situated in the N-terminal part of the protein, and according to a domain analysis, the N terminus of HCAI (residues 1−25) has few contacts with the rest of the molecule (Janin & Wodak, 1983). Since HCAII and HCAI have very similar three dimensional structures (Eriksson et al., 1988; Kannan et al., 1975, 1984), the N terminus of HCAII should also form a small domain. Trp96 is located in the hydrophobic core, and Trp245 is positioned in a loop at the interface of the N-terminal and the major domains. Furthermore, these Trp's are also the major contributors to the near-UV CD spectrum (Freskgård et al., 1994), and the fluorescence of Trp16 has been shown to monitor the slowest phase in the refolding of $HCAII_{pwt}$ (Aronsson et al., 1995), which are the major characteristics that made this study feasible. In addition, Trp97 and -245 are the major fluorescence emitters in the native structure (Mårtensson et al., 1995).

We have recently shown, by two-dimensional NMR of ^{15}N-labled Trp mutants, that single mutations of the seven Trp residues of $HCAII_{pwt}$ had essentially no long-range effects on structure (Mårtensson et al., 1995). CD measurements of the mutants lacking one Trp residue also corroborate this conclusion, since the sum of the individual Trp CD spectra obtained from the mutants was used to reconstruct the $HCAII_{pwt}$ near-UV CD spectrum reasonably well (Freskgård et al., 1994). These observations strongly indicate that the mutations have no or minor effects on the remaining Trp residues in the native state. Neither do the substitutions made in the mutants seem to have any large influence on the overall refolding properties, as judged from the similar magnitudes of the rate constants describing the kinetics of the reactivation (as probed by the binding of the active site inhibitor DNSA, Table 2).

The binding of the active site inhibitor, DNSA, and the slow formation of the asymmetric substructures around the Trp residues in the enzyme during the folding process were in each case best described by two exponential phases for $HCAII_{pwt}$ (Tables 2 and 3). In addition, the intrinsic fluorescence change during the refolding of $HCAII_{pwt}$ also contains two phases with rate constants with similar magnitudes (Aronsson et al., 1995).

The individual CD spectra of each Trp residue exhibit a unique pattern during the whole time course of refolding, which is strong evidence that the developing spectra mainly emanate from the particular Trp residue under study and that the spectra reflect formation of native-like tertiary interactions in the substructure around the particular Trp (Figure 4A−C).

Initial Formation of Asymmetric Substructures. About one-third of the total CD change at 270 nm for Trp97 has already occurred during the first minute of refolding (Figure 6; mean value of ellipticity of -26 ± 1 deg cm^2 dmol^{-1}), indicating that there also exists a minor population of protein molecules in which local native-like structures are formed within 1 min, which is before the events that we are characterizing. Notably, the corresponding value for the reactivation (or inhibitor-binding capacity) of the W97C mutant after the same time interval (1 min) is only 14%. Evidently, local native-like structure is formed that lacks

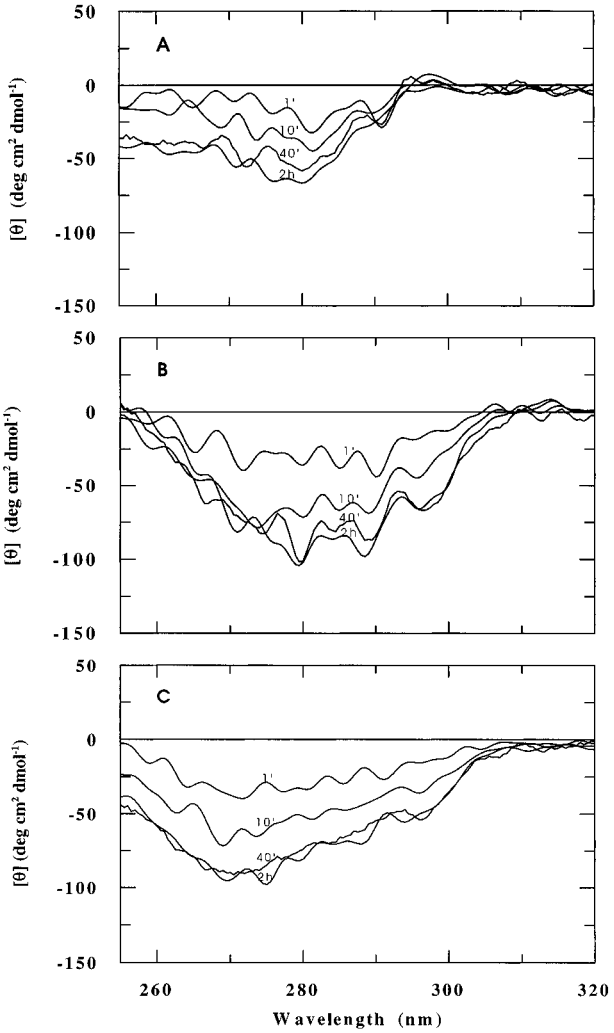

FIGURE 4: Development of individual near-UV CD Trp spectra during refolding. The CD spectra of an individual Trp were obtained by subtraction of the CD spectra of the corresponding Trp mutant from the CD spectra of $HCAII_{pwt}$ at the same time point during refolding. The time when the scan was started after the onset of refolding is indicated together with each spectrum: (A) Trp16, (B) Trp97. and (C) Trp245.

enzymatic activity. The initial CD change (1 min) of Trp245 (-14 ± 1 deg cm^2 dmol^{-1}) is on the other hand equivalent to the degree of reactivation.

Formation of Tertiary Structure in the N-Terminal Region. After 1 min of refolding (the starting value), no significant difference between the ellipticity at 270 nm of $HCAII_{pwt}$ and the W16F mutant is observed (Figure 5), whereas after 2 h of refolding, this difference in ellipticity has grown to 56 deg cm^2 dmol^{-1} (Figures 5 and 6). This shows that there is almost no immobilization of the side chain of Trp16 within the first minute. Subsequently, the Trp16 residue is gaining its native structural environment, according to the development of the near-UV CD signal, at a rate 2.9 times slower than the formation of the active site in the first population of refolding molecules and 6 times slower in the second population (kinetic phases 1 and 2, respectively, in Tables 2 and 4). Trp16 is situated in the N-terminal domain of the protein (Figure 1). This part of the molecule is highly exposed to solvent. Moreover, the N-terminal domain can be removed without disrupting the native (active) structure of the major domain (Aronsson et al., 1995). In agreement with previous fluorescence results

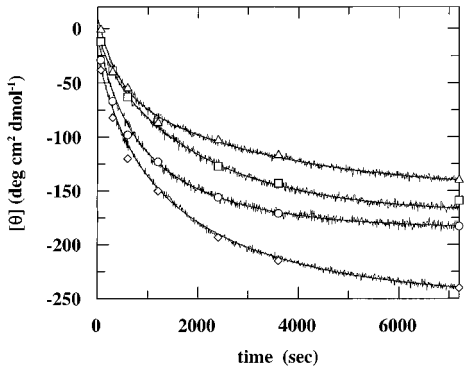

FIGURE 5: Kinetics of ellipticity changes during refolding of $HCAII_{pwt}$ and mutants lacking one Trp residue. The refolding reaction was monitored continuously at a fixed wavelength, 270 nm. The symbols indicate the values at 270 nm taken from the CD spectra shown in Figure 3. The kinetic traces are from one representative experiment of each protein variant. Symbols and rate constants for each curve are as follows (mean values are shown in Table 3): (◇) $HCAII_{pwt}$ ($k_1 = 1.7 \times 10^{-3}$ s^{-1}; $k_2 = 0.4 \times 10^{-3}$ s^{-1}), (○) W16F/C206S mutant ($k_1 = 2.0 \times 10^{-3}$ s^{-1}; $k_2 = 0.5 \times 10^{-3}$ s^{-1}), (□) W97C/C206S mutant ($k_1 = 2.8 \times 10^{-3}$ s^{-1}; $k_2 = 0.5 \times 10^{-3}$ s^{-1}), and (Δ) W245C/C206S mutant ($k_1 = 2.6 \times 10^{-3}$ s^{-1}; $k_2 = 0.3 \times 10^{-3}$ s^{-1}).

Table 3: Kinetic Data for the Refolding of $HCAII_{pwt}$ and Tryptophan Mutants Thereof as Monitored by Circular Dichroism at 270 nm[a]

variant	k_1[b] ($\times 10^3$ s^{-1})	A_1[b]	k_2[b] ($\times 10^3$ s^{-1})	A_2[b]	yield[c] (%)
C206S	1.7 ± 0.1	94 ± 7	0.47 ± 0.03	134 ± 6	69 ± 3
W16F/C206S	2.2 ± 0.2	69 ± 2	0.56 ± 0.04	103 ± 2	63 ± 2
W97C/C206S	3.0 ± 0.5	25 ± 3	0.36 ± 0.03	161 ± 11	63 ± 5
W245C/C206S	2.8 ± 0.2	56 ± 4	0.33 ± 0.04	96 ± 1	69 ± 3

[a] The protein variants were denatured in 5 M GuHCl and then refolded by dilution to 0.15 M GuHCl. [b] The rate constants and amplitudes were calculated using a nonlinear fit program (see Materials and Methods). The rate constants and amplitudes are mean values with standard mean deviations and are based on quadruplicate refolding experiments. [c] The mean value with standard deviations of the yield of the refolded protein calculated from the ellipticity change.

(Aronsson et al., 1995), these CD data clearly indicate that the formation of the N-terminal domain is dependent on the prior formation of an enzymatically active native-like conformation of the rest of the protein. The major domain presumably acts as a template for the correct folding of the N-terminus.

Formation of Tertiary Structure in the Major Domain. After the initial "burst" phase (1 min), Trp97 regains its CD spectral bands relatively slowly during the refolding reaction (Figure 6, Table 4). Trp97 is located in β-strand 4 (Figure 1) and is included in a hydrophobic cluster which consists of 32 amino acid residues, eight of which are aromatic (Eriksson et al., 1988). Previously, we have shown that this region of the molecule, including β-strands 3−5, is remarkably stable and compact and is not unfolded until extremely strong denaturing conditions (>5 M GuHCl) are applied. This part of the molecule probably represents an initiation site of folding (Mårtensson et al., 1993; Svensson et al., 1995). Furthermore, recent stopped-flow fluorescence data indicate that Trp97 is buried in a compact apolar cluster with essentially a native-like compactness within a few milliseconds (Jonasson et al., 1997). However, the groups surrounding Trp97 in this compact state evidently rearrange

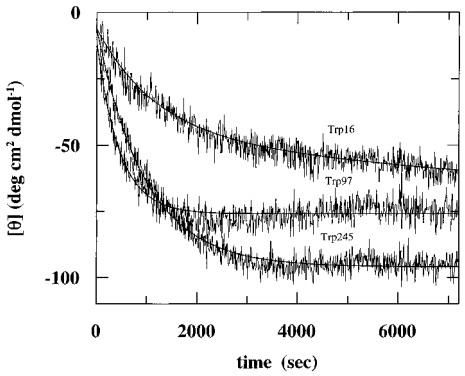

FIGURE 6: Kinetics of ellipticity changes during refolding of individual Trp residues in $HCAII_{pwt}$. The kinetic trace of the specific Trp was obtained by subtraction of the trace from the corresponding mutant lacking this Trp residue from that of $HCAII_{pwt}$. The kinetic traces are from one representative experiment. The corresponding rate constants calculated from each curve are as follows (mean values are shown in Table 4): Trp16 ($k_1 = 0.8 \times 10^{-3}$ s^{-1}; $k_2 = 0.1 \times 10^{-3}$ s^{-1}), Trp97 ($k_1 = 2.2 \times 10^{-3}$ s^{-1}), and Trp245 ($k_1 = 0.8 \times 10^{-3}$ s^{-1}).

Table 4: Kinetic Data Obtained from the Reappearance of the CD Signal at 270 nm of Individual Tryptophan Residues in $HCAII_{pwt}$ during Refolding[a]

Trp residue	k_1[b] ($\times 10^3$ s^{-1})	A_1[b]	k_2[b] ($\times 10^3$ s^{-1})	A_2[b]
16	0.8 ± 0.1	32 ± 5	0.11 ± 0.07	40 ± 8
97	2.3 ± 0.2	55 ± 4	−[c]	−[c]
245	0.8 ± 0.1	83 ± 2	−[c]	−[c]

[a] The protein variants were denatured in 5 M GuHCl and then refolded by dilution to 0.15 M GuHCl. [b] The rate constants and amplitudes were calculated using a nonlinear fit program (see Materials and Methods). The rate constants and amplitudes are mean values with standard mean deviations. [c] The kinetic data for this Trp residue were best fitted to a monophasic reaction.

to a native-like tertiary structure on a significantly slower time scale according to the CD data.

Moreover, Trp97 is located in one of the active site walls and together with Phe93 and Phe95 enclose the zinc ligands His94 and His96 (Eriksson et al., 1988). Since the rate of reappearance of inhibitor binding capacity during refolding is similar to that of recovery of the native CD spectrum of Trp97 (Tables 2 and 4), Trp97 thus seems to probe the formation of a functioning active site structure. Apparently, formation of the native tertiary structure in the hydrophobic cluster is tightly coupled to the formation of native structure on the upper half of the central β-sheet (Figure 1). The biphasic kinetics noted for the formation of an inhibitor-binding active site (Table 2) might depend on formation of other parts of the molecule. We have earlier shown that proline isomerization is the cause of slow reactivation kinetics of HCAII. Thus, the observation of slow kinetic phases is probably due to proline isomerization steps (Fransson et al., 1992).

Trp245 is situated in a long loop at the interface of the N-terminal and the major domains (Figure 1). We have previously also shown that the loop containing Trp245 appears to be held together with the rest of the hydrophobic core in an equilibrium folding intermediate of molten-globule character that is stable at moderate GuHCl concentrations (Svensson et al., 1995). Although Trp245 has acquired native-like fluorescence properties (Aronsson et al., 1995) within the dead time of the CD experiment, it assumes, according to the CD data, a native-like tertiary structure even slower than Trp97 (Figure 6, Table 4). Thus, the investigated Trp residues develop their native CD bands at different rates, showing that formation of native-like tertiary structure is occurring with varying rates in different regions of the protein.

Evidently, the Trp residues report different rates depending on whether the refolding process is monitored by CD or fluorescence measurements. However, these contrasting observations need not be contradictory, since fluorescence and CD measurements are probing different physical properties. Changes in intrinsic fluorescence of the Trp residues 97 and 245 during the refolding process reflect changes in polarity only, while CD measurements reflect changes in asymmetric properties of the substructures around the inspected Trp residues.

Intrinsic fluorescence and near-UV CD characteristics thus provide complementary information regarding the behavior of aromatic side chains during the folding process. In general, interpretation of CD data is rather straightforward, while interpretation of fluorescence data sometimes is more complicated due to physical factors such as energy transfer and quenching. The specific CD bands in the near-UV region are very sensitive to conformational changes, and therefore, the near-UV CD spectrum can be used as a fingerprint of the native conformation.

ACKNOWLEDGMENT

We thank Göran Aronsson (Umeå University) for making Figure 1.

REFERENCES

Aronsson, G., Mårtensson, L.-G., Carlsson, U., & Jonsson, B.-H. (1995) *Biochemistry 34*, 2153−2162.
Bashford, D., Chothia, C., & Lesk, A. M. (1987) *J. Mol. Biol. 196*, 199−216.
Behravan, G., Jonsson, B.-H., & Lindskog, S. (1991) *Eur. J. Biochem. 195*, 393−396.
Chen, R. F., & Kernohan, J. C. (1967) *J. Biol. Chem. 242*, 5813−5823.
Craig, S., Pain, R. H., Schmeisser, U., Virden, R., & Wingfield, T. P. (1989) *Int. J. Pept. Protein Res. 33*, 256−262.
Eriksson, A. E., Jones, T. A., & Liljas, A. (1988) *Proteins: Struct., Funct., Genet. 4*, 274−282.
Fransson, C., Freskgård, P.-O., Herbertsson, H., Johansson, Å., Jonasson, P., Mårtensson, L.-G., Svensson, M., Jonsson, B.-H., & Carlsson, U. (1992) *FEBS Lett. 296*, 90−94.
Freskgård, P.-O., Carlsson, U., Mårtensson, L.-G., & Jonsson, B.-H. (1991) *FEBS Lett. 289*, 117−122.
Freskgård, P.-O., Bergenhem, N., & Carlsson, U. (1992) *Anal. Chim. Acta 269*, 143−148.
Freskgård, P.-O., Mårtensson, L.-G., Jonasson, P., Jonsson, B.-H., & Carlsson, U. (1994) *Biochemistry 33*, 14281−14288.
Gill, S. C., & von Hippel, P. H. (1989) *Anal. Biochem. 182*, 2083−2093.
Goldberg, M. E., Semisotnov, G. V., Friguet, B., Kuwajima, K., Ptitsyn, O. B., & Sugai, S. (1990) *FEBS Lett. 263*, 51−56.
Håkansson, K., Carlsson, M., Svensson, L. A., & Liljas, A. (1992) *J. Mol. Biol. 227*, 1192−1204.
Henkens, R. W., Kitchell, B. B., Lottisch, S. C., Stein, P. J., & Williams, T. J. (1982) *Biochemistry 21*, 5918−5923.
Janin, J., & Wodak, S. J. (1983) *Prog. Biophys. Mol. Biol. 42*, 21−78.
Jonasson, P., Aronsson, G., Carlsson, U., & Jonsson, B.-H. (1997) *Biochemistry 36* (in press).
Kannan, K. K., Notstrand, B., Fridborg, K., Lövgren, S., Ohlsson, A., & Petef, M. (1975) *Proc. Natl. Acad. Sci. U.S.A. 72*, 51−55.
Kannan, K. K., Ramanadham, M., & Jones, T. A. (1984) *Ann. N.Y. Acad. Sci. 429*, 49−60.

Khalifah, R. G., Strader, D. J., Bryant, S. H., & Gibbons, S M. (1977) *Biochemistry 16*, 2241−2247.
Kraulis, P. (1991) *J. Appl. Crystallogr. 24*, 946−950.
Krebs, J. F., & Fierke, C. A. (1993) *J. Biol. Chem. 268*, 948−954.
Lim, W. A., & Sauer, R. T. (1991) *J. Mol. Biol. 219*, 359−376.
Mårtensson, L.-G., Jonsson, B.-H., Andersson, M., Kihlgren, A., Bergenhem, N., & Carlsson, U. (1992) *Biochim. Biophys. Acta 1118*, 179−186.
Mårtensson, L.-G., Jonsson, B.-H., Freskgård, P.-O., Kihlgren, A., Svensson, M., & Carlsson, U. (1993) *Biochemistry 32*, 224−231.
Mårtensson, L.-G., Jonasson, P., Freskgård, P.-O., Svensson, M., Carlsson, U., & Jonsson, B.-H. (1995) *Biochemistry 34*, 1011−1021.
Nozaki, Y. (1972) *Methods Enzymol. 26*, 43−50.
Nyman, P. O., & Lindskog, S. (1964) *Biochim. Biophys. Acta 85*, 141−151.
Ptitsyn, O. B., Pain, R. H., Semisotnov, G. V., Zerovnik, E., & Razgulyaev, O. I. (1990) *FEBS Lett. 262*, 20−24.
Sandberg, W. S., & Terwilliger, T. C. (1991) *Proc. Natl. Acad. Sci. U.S.A. 88*, 1706−1710.
Semisotnov, G. V., Rodinova, N. A., Kutyshenko, V. P., Ebert, B., Blank, J., & Ptitsyn, O. B. (1987) *FEBS Lett. 224*, 9−13.
Semisotnov, G. V., Uversky, V. N., Sokolovsky, I. V., Gutin, A. M., Razgulyaev, O. I., & Rodinova, N. A. (1990) *J. Mol. Biol. 213*, 561−568.
Svensson, M., Jonasson, P., Freskgård, P.-O., Jonsson, B.-H., Lindgren, M., Mårtensson, L.-G., Gentile, M., Borén, K., & Carlsson, U. (1995) *Biochemistry 34*, 8606−8620.
Thorslund, A., & Lindskog, S. (1967) *Eur. J. Biochem. 3*, 117−123.
Vuilleumier, S., Sancho, J., Loewenthal, R., & Fersht, A. R. (1993) *Biochemistry 32*, 10303−10313.

BI961925N